International Journal of Thermophysics, Vol. 23, No. 1, January 2002 (© 2002)

Zirconium and Iron Densities in a Wide Range of Liquid States[1]

V. N. Korobenko,[2] M. B. Agranat,[2] S. I. Ashitkov,[2] and A. I. Savvatimskiy[2, 3]

Metals (Fe, Zr) were investigated under a 1-bar air ambient atmosphere. Electrical pulse current heating was applied to iron and zirconium wires for 5 to 7 μs. The specimens were shadowgraphed by a pulse laser with a duration of $\tau \approx 6$ ns. The shadow picture was then transmitted to a digital CCD camera and subjected to digital photometrical processing. The differences between the measured and the known literature values for liquid iron density are 1 to 6%, which shows that this new method is appropriate. The dependences of resistivity on the specific imparted energy were obtained for the liquid state of Fe and Zr. With the examples of iron and zirconium, the possibility of using the proposed method to obtain reliable data for the thermal expansion of liquid metals and the electrical resistivity over a wide range of the liquid phase is demonstrated.

KEY WORDS: density; expansion; fast heating; high temperature; iron; liquid state; resistivity; zirconium.

1. INTRODUCTION

The measurement of time-dependent thermal expansion of liquid metals is performed by means of electric current pulse heating of wire specimens up to temperatures much higher than the melting point. The method for obtaining the liquid metal is to heat up a cylindrical wire 100 to 200 μm in diameter, d ($d \ll l$, where l is the wire length). During the period of heating, the wire expands in the liquid phase laterally, but not longitudinally, as it is fixed at both ends.

[1] Paper presented at the Fourteenth Symposium on Thermophysical Properties, June 25–30, 2000, Boulder, Colorado, U.S.A.

[2] Institute of High Energy Density (IHED), United Institute for High Temperature, Russian Academy of Sciences, Izhorskaya 13/19, 127412 Moscow, Russia.

[3] To whom correspondence should be addressed. E-mail: savlab@iht.mpei.ac.ru

0195-928X/02/0100-0307/0 © 2002 Plenum Publishing Corporation

A digital CCD camera with an exactly defined time delay obtains a shadow picture of the wire diameter. The duration of a laser pulse shadowgraph τ_p, while being measured by a digital videocamera, is determined by a minimum temperature interval of measurements and a temperature increment rate (in our case the temperature increment rate is $\approx 10^{10}$ K · s^{-1}; thus, $\tau_p \approx 10$ ns corresponds to a temperature interval of 10 K).

2. EXPERIMENTAL

2.1. Optical Scheme of the Measurement Method

The optical scheme of measurements is as follows. The surveyed area is shadowgraphed by a second-harmonic pulsed Nd:YAG laser with a wavelength $\lambda = 530$ nm and a duration of 6 ns. The surveyed object is a wire either 200 μm in diameter (Fe) or 180 μm in diameter (Zr) and 30 mm long. It is heated with an electric current pulse 5 to 7 μs in duration. The shadow picture of the wire is transmitted to a digital CCD camera input with a magnification power of 10. A narrow-band interference filter and a set of color and neutral light filters suppresses thermal radiation of the heated wire. A control unit synchronizes the current and laser pulses to the CCD camera and, thus, provides variable time delay of the shadowgraph over the current heating pulse.

Figure 1 shows a characteristic picture obtained with the digital videocamera. The spatial resolution of the CCD camera along the abscissa axis (lateral dimensions of the wire) is 6 μm (size of the pixel).

Since the magnification factor is 10, the spatial resolution at the object is about 0.6 μm. This is greater than the laser pulse shadowgraph wavelength, and the optical system is capable of providing such a resolution. The assessment of the results has shown that it is possible to process image dimensions with an uncertainty of nearly 1 μm.

2.2. Current Heating Method and Measurement of the Imparted Energy Value

The capacitor bank with a stored energy of 25 kJ was discharged through the specimen and a ballast resistor connected in series. To measure the total current running through the wire, a Rogovsky coil was used. The procedure to calibrate the Rogovsky coil implied recording of the current (with an amplitude of up to 10 kA) through a shunt with known parameters (impedance, 0.03 Ω; inductance, 0.12 nH) and comparison of signals

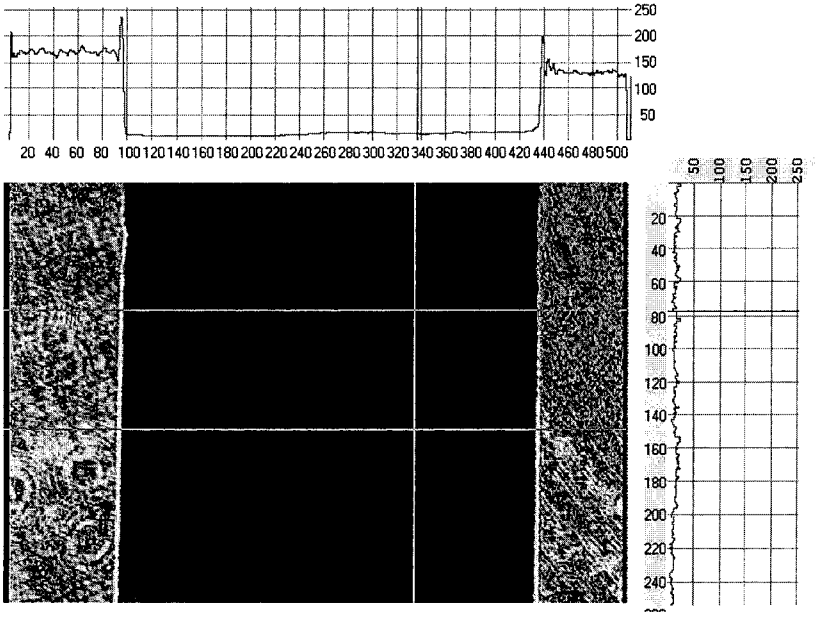

Fig. 1. Image of the wire diameter (0.2 mm), horizontal axes, from the CCD camera. The dependence (in arbitrary units): (top) digital photometrical processing of the shadow picture *across* the wire and (right) digital photometrical processing of the shadow picture *along* the wire.

at the current shunt and the Rogovsky coil using a digital oscilloscope (Tektronix 754C). The deviation of the conversion coefficient of the Rogovsky coil constant did not exceed 1.5% in the area where the current change rate did not exceed 5×10^9 $A \cdot s^{-1}$ within 10 μs of the current run. To measure the voltage across the specimen, an ohmic voltage divider was used. The attenuation was determined with an uncertainty of 0.1% with respect to the direct current.

To record a laser pulse, a photoreceiver was used. The basic component of the photoreceiver is a silicon PIN photodiode with quartz optical fiber. The photoreceiver rise time was less than 10 ns, and the dynamic range was 600 at 0 to 50 MHz. The maximum deviation from linear dependence of the voltage output signal from the radiation input signal was less than 5% over the complete dynamic range of the photoreceiver.

The length of Zr wire (about 1 m) was determined with an uncertainty of about 0.1%. The mass of the specimen could be measured with an uncertainty of about 0.5%. The specimen was weighed in air and in boiled (degassed) water, and a density of 6.505 $g \cdot cm^{-3}$ at room temperature was

obtained for Zr. The electrical resistance of a specimen was determined by the equation

$$R(t) = [U(t) - L(dI/dt)]/I(t) \tag{1}$$

where U is the voltage at the specimen, L is the inductance of the specimen, and I is the current running through the specimen. Calculation of the specimen inductance L gives a value 13% higher when the specimen's volume doubles. The total error in the R determination is 3% for the case $dI/dt \leqslant 10^9\ \mathrm{A \cdot s^{-1}}$. The electrical resistivity of the specimen is calculated by

$$\rho(t) = R(t)\, S/l \tag{2}$$

where S is the cross-sectional area of the expanding specimen and l is the specimen length. The amount of the energy E absorbed per unit of mass is

$$E(t) = \int_0^t [I^2(t) \cdot R(t)/m]\, dt \tag{3}$$

where m is the mass of the specimen. The estimated uncertainty in determining E is about 4% near the melting point. The absolute error of measurement of the heated wire diameter (d) by a CCD camera was 1 μm (without processing of the image edge diffraction picture). Taking into account that the volume is proportional to d^2, the measurement error of the expanded specimen diameter (volume) will be 1.4 μm.

The impurities (mass percentage) of the Zr wire of 0.18-mm diameter are as follows: Fe, Hf, O_2—and 0.05% each; Nb and C—0.03% each; Al, Si, Ti, and Cu—0.005% each; and N_2—0.01%.

3. MEASUREMENTS ON LIQUID IRON

3.1. Experimental Results

The measurement methodology was tested using iron specimens (steel with a carbon content of about 0.1%). The wire had a diameter of 200 μm. The diameter of the wire and the iron density were determined again. A specimen about 1 m long was weighed on an analytical balance (with an uncertainty of 0.15 mg), first in air and then in degassed water. The measured initial density of iron appeared to be $7.87\ \mathrm{g \cdot cm^{-3}}$. The length of the specimens subjected to heating was 30 mm (with an uncertainty of up to 50 μm). Figure 2 shows the results of an expansion of iron wire obtained with 16 specimens. Each specimen is represented by a square in Fig. 2.

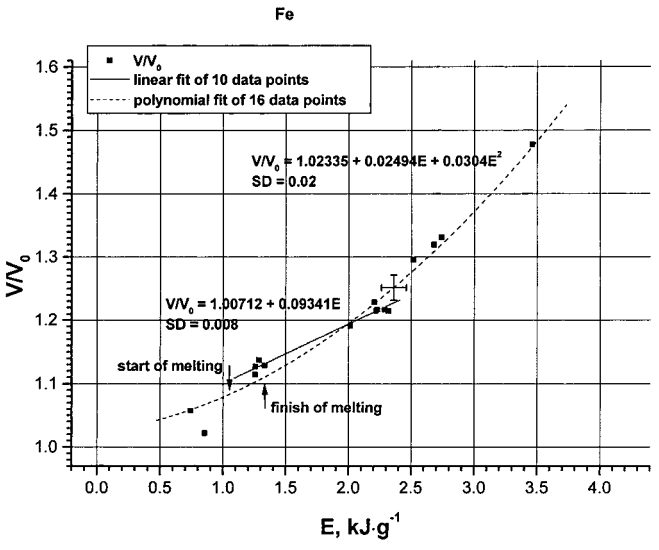

Fig. 2. Thermal expansion of Fe versus specific imparted energy. The start (1.06 $kJ \cdot g^{-1}$) and the end (1.33 $kJ \cdot g^{-1}$) of iron melting are shown by arrows, according to Ref. 1. Squares, our data: dashed curve, polynomial fit over all 16 data points; solid curve, linear fit of the data in a narrow liquid-phase region (10 points). The ordinate axis represents the relative change of volume V/V_0, and the abscissa axis represents the specific imparted energy E (starting from the room-temperature level). The error in specific imparted energy and volume change is given for one of the imparted energy values (close to 2.5 $kJ \cdot g^{-1}$).

Figure 3 provides the results of measurements of the liquid iron density versus the specific imparted energy E compared to the literature values. According to our data (Figs. 2 and 3), the average temperature coefficient of the volumetric expansion (β) of liquid iron from the melting point, 1810 K, to the boiling point, 3148 K [2] (at ≈ 2.5 $kJ \cdot g^{-1}$), is $\sim 102 \times 10^{-6}$ K^{-1}. The latter value is close to the data for Fe in Ref. 3 ($\beta = 91.5 \times 10^{-6}$ K^{-1}, linear up to 2300 K) and to the data in Ref. 4 ($\beta = 115.1 \times 10^{-6}$ K^{-1} for liquid steel with 0.12% C).

3.2. Experimental Procedure for the Calculations of One Shot (Fe-18)

As an example of how this methodology was used to obtain the electrical resistivity of liquid iron, we provide the data from one single experiment (Fe-18) in Fig. 4. Figure 4 gives the current and voltage values at the

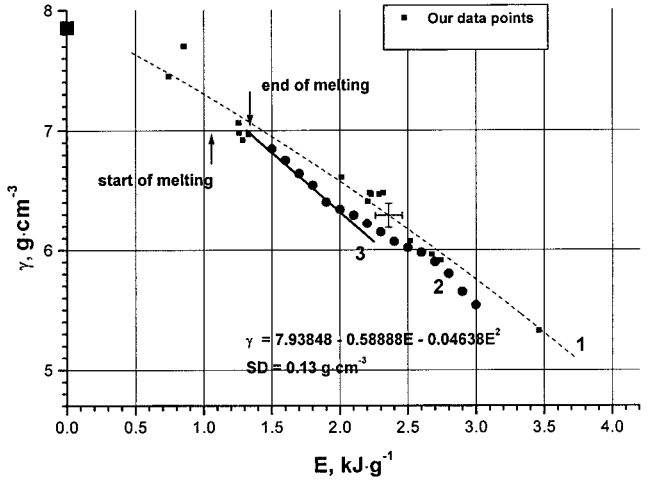

Fig. 3. Density of Fe versus specific imparted energy. The start (1.06 kJ·g^{-1}) and the end (1.33 kJ·g^{-1}) of iron melting are shown by arrows, according to Ref. 1. Squares—our data; the initial point is shown at $E = 0$. Dashed curve—polynomial fit of all our data. The error in density and imparted energy measurement is given for the value close to 2.5 kJ·g^{-1}. Dashed curve (1)—our data for solid and liquid iron, obtained in air. The full time of heating was 10 μs. Circles (2)—data from Ref. 5 for liquid iron, obtained under a high argon pressure (2 kbar). According to Ref. 5, $E = 3$ kJ·g^{-1} corresponds to 3950 K. Solid line (3)—data from Ref. 6 for liquid iron, obtained in water under a high pressure (up to 3.8 kbar). The full time of heating in Ref. 6 was 55 μs. According to Ref. 6, $E = 3$ kJ·g^{-1} corresponds to 3861 K (accordingly, $E = 3.75$ kJ·g^{-1} at 4770 K).

specimen and a laser flash, shadowgraphed just at the moment when the melting was finished (at an imparted energy of 1.33 kJ·g^{-1}). Figure 5 shows the reduced electrical resistivity ρ_0 (referenced to the specimen dimensions at room temperature) and the specific electrical resistivity ρ, for which the thermal expansion with regard to the experimental data for 10 specimens shown in Fig. 2 was taken into account versus the energy. At the melting point ($E = 1.33$ kJ·g^{-1}), ρ is equal to $\rho_0 \times V/V_0$, where the increase in volume of 13% is taken into account according to the linear fit of the data in Fig. 2. The density of liquid iron is 6.95 g·cm^{-3} (linear fit near melting point; Fig. 2) or 7.05 g·cm^{-3} (polynomial fit of all our data; Fig. 3) from our measurements at the end of melting.

The electrical resistivity of liquid iron as a function of temperature may be obtained. Taking into account the heat capacity of liquid iron as a

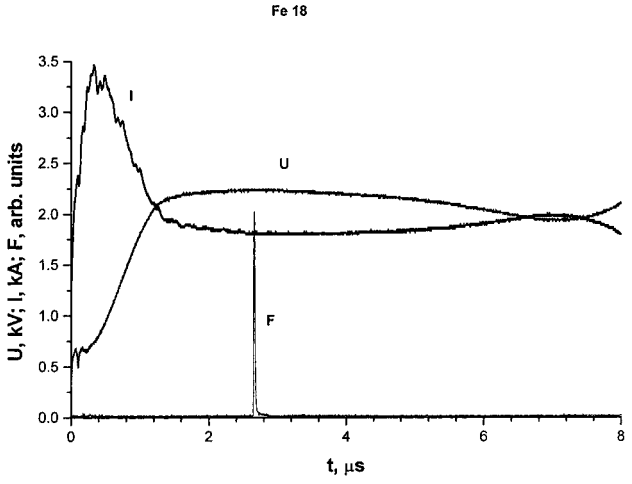

Fig. 4. Initial experimental data (current I and voltage U versus time t) for one of our experiments. The laser flash (F) is shown, just at the end of Fe melting (1.33 $kJ \cdot g^{-1}$, according to Ref. 1).

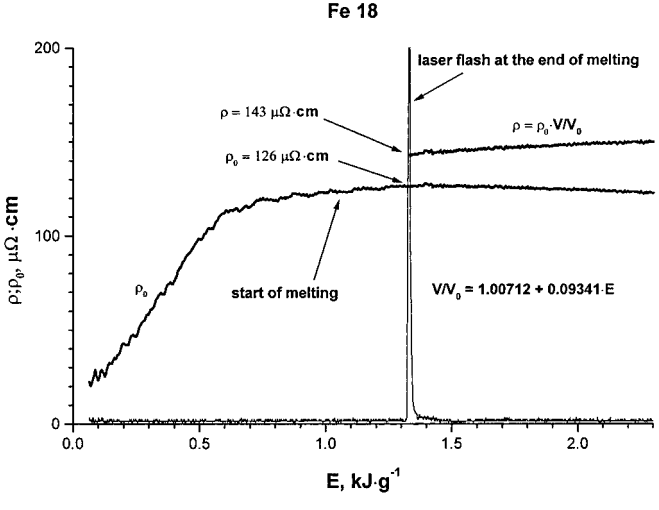

Fig. 5. Electrical resistivity of Fe versus specific imparted energy. ρ_0—electrical resistivity referenced to initial dimensions of the specimen (126 $\mu\Omega \cdot$cm for the liquid phase at the melting point). $\rho = \rho_0 \times V/V_0$ —electrical resistivity with thermal expansion taken into account (143 $\mu\Omega \cdot$cm for the liquid phase at the melting point). Volume dependence V/V_0 versus E is shown.

constant, $c_p = 0.786\ \mathrm{J \cdot g^{-1} \cdot K^{-1}}$ [2, 5], one can obtain the electrical resistivity of liquid iron as $\sim 150\ \mu\Omega \cdot \mathrm{cm}$ at the boiling point, 3148 K [2], at an imparted energy of $\approx 2.5\ \mathrm{kJ \cdot g^{-1}}$. Under the maximum imparted energy ($3.5\ \mathrm{kJ \cdot g^{-1}}$), an unleveled edge of the liquid iron cylinder is seen in the photograph. Perhaps this is connected with the iron boiling at the temperature $T = 4500$ K.

3.3. Summary of Density Measurements of Liquid Metals (Fe and Steels)

The well-known book by Wilson [2] gives the value of the electrical resistivity of liquid iron at the melting point as $138.6\ \mu\Omega \cdot \mathrm{cm}$. The heat capacity of liquid iron is $c_p = 0.786\ \mathrm{J \cdot g^{-1} \cdot K^{-1}}$ [2].

For the case of liquid steel with a carbon content of 0.13%, the formulas to calculate the electrical resistivity at temperatures up to 1923 K are given in Ref. 4:

$$\rho = 135.1[1 + 2.88 \times 10^{-4}](T - 1810\ \mathrm{K}),$$
$$\rho = 145.5[1 + 3.14 \times 10^{-4}](T - 1810\ \mathrm{K}) \tag{4}$$

Experimental data on liquid iron were obtained in Ref. 6 with 55-μs electrical pulse heating. Iron wires were heated in water, under a high pressure (up to 3.8 kbar). Reference 6 reports data up to 4770 K ($E = 3.75\ \mathrm{kJ \cdot g^{-1}}$), but the density was obtained only to 2952 K ($E = 2.25\ \mathrm{kJ \cdot g^{-1}}$); see Fig. 3. The specific heat capacity is $0.825\ \mathrm{kJ \cdot g^{-1} \cdot K^{-1}}$ [6].

Experimental data on liquid iron were obtained in Ref. 5 by fast electrical pulse heating under a high argon pressure (2 kbar). Data on density were obtained up to 3950 K ($E = 3.0\ \mathrm{kJ \cdot g^{-1}}$). These data are shown in Fig. 3. According to Ref. 5, the average volume expansion coefficient is $\beta = 93 \times 10^{-6}$ near a density of $\gamma = 7.1\ \mathrm{g \cdot cm^{-3}}$ and $\beta = 115 \times 10^{-6}$ near a density of $\gamma = 5.7\ \mathrm{g \cdot cm^{-3}}$, and the specific heat capacity is $0.815\ \mathrm{kJ \cdot g^{-1} \cdot K^{-1}}$ [5].

Steady-state experimental data were published in Ref. 3 for the density of liquid iron at temperatures up to 2300 K. The data were obtained by means of a γ-densitometer. Within the temperature range 1810 to 2300 K, the density of liquid iron is a linear function of temperature. At the melting point, the density of iron is about $7\ \mathrm{g \cdot cm^{-3}}$ [3], and at a temperature of 2300 K, it is about $6.7\ \mathrm{g \cdot cm^{-3}}$. The average temperature coefficient of the volumetric expansion of liquid iron is $\beta = 91.4 \times 10^{-6}\ \mathrm{K^{-1}}$.

4. MEASUREMENTS ON LIQUID ZIRCONIUM

4.1. Summary of Literature Data

According to Ref. 7, an approximate equation to calculate the density γ of liquid zirconium "at different temperatures" was proposed in 1956 [8]:

$$\gamma = 6.0 - (T - 2123) \times 10^{-3} \ (\mathrm{g \cdot cm^{-3}}) \tag{5}$$

Reference 7 does not indicate up to what temperature this equation is valid. The authors indicated that the result (6.06 to 6.08 $\mathrm{g \cdot cm^{-3}}$) was given "at the temperature close to the melting temperature [7]" for zirconium containing 0.5% carbon.

According to Ref. 9, the density of liquid zirconium at the melting point is 5.95 $\mathrm{g \cdot cm^{-3}}$. In 1983, the expansion of liquid zirconium (wire of 1 mm in diameter) was measured [10] under pulse heating. These measurements were reported as preliminary. The measurements were done in a high-pressure gas vessel (3 kbar). For the case of a single experiment, the dependence of the expansion of zirconium on the imparted energy was obtained (Fig. 6).

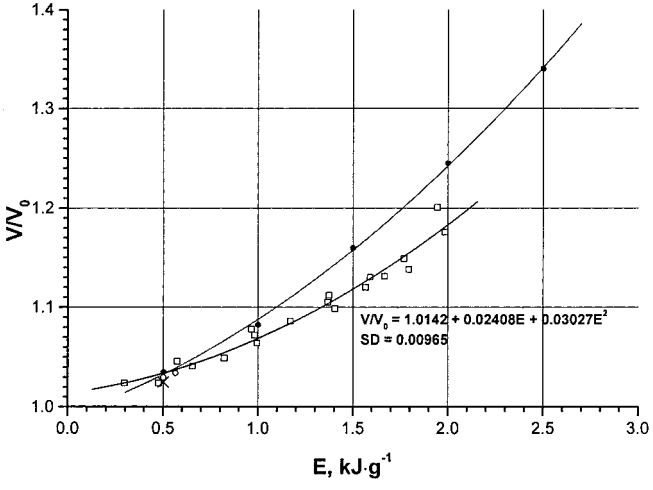

Fig. 6. V/V_0 versus imparted energy for zirconium. Open squares and polynomial fit—our data. The standard deviation (SD) is shown. Filled circles and polynomial fit—data from Ref. 10. Two open circles near 0.5 $\mathrm{kJ \cdot g^{-1}}$—data from Ref. 13. Cross under imparted energy, 0.5 $\mathrm{kJ \cdot g^{-1}}$—from Ref. 14.

For the solid phase of zirconium, the average linear thermal expansion coefficient $\alpha = 7.5 \times 10^{-6}$ K^{-1} (300 to 1000 K) [11] and $\alpha = 8.0 \times 10^{-6}$ K^{-1} ($T = 593$ to 1093 K) [12].

4.2. Measurement Results on Liquid Zirconium Density

The measurements carried out for liquid zirconium (similarly to the measurements for liquid iron) produced the following result (Fig. 6). This shows the ratio of the specific volume of zirconium to its initial specific volume, V/V_0, depending on the specific imparted energy E. The open squares and fitted curve represent our data. The curve obtained in this work is slightly below that of Ref. 10. According to our data (Fig. 6), at the start of the liquid state ($E \cong 0.85$ kJ$\cdot$g^{-1}), the expansion V/V_0 is $\sim 5.7\%$, while Ref. 10 reports 7%. During melting ($E_1 \cong 700$ J$\cdot$g^{-1} and $E_2 \cong 850$ J$\cdot$g^{-1}), the volume increases only 1.2%, while Ref. 9 recommends 5%. It should be mentioned for comparison that the expansion of iron at melting is 3% according to our data obtained by the same technique. The published data for the volume increase at melting provide values of from 1 to 3.5% for iron at the melting point. For the two points mentioned above ($E = 0.85$ kJ$\cdot$g^{-1} and $E = 2.0$ kJ$\cdot$g^{-1}), the density of liquid zirconium is 6.12 and 5.55 g$\cdot$cm^{-3}, respectively (Fig. 7).

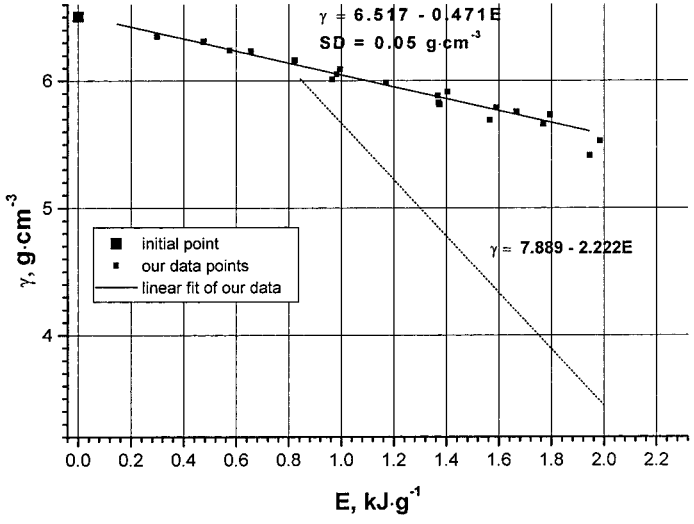

Fig. 7. Density versus imparted energy for solid (up to ~ 0.7 kJ$\cdot$g^{-1}) and liquid (above ~ 0.85 kJ$\cdot$g^{-1}) zirconium. Squares—our data, with a linear fit. The standard deviation (SD) is shown. Dotted line—estimates from Ref. 7 for liquid Zr.

5. DISCUSSION

According to our estimations the conditions of the Zr wire being heated by an electrical current for $\sim 7\,\mu s$ up to energies of $\sim 2\ kJ \cdot g^{-1}$ (duration of heating up to melting is $\sim 3\,\mu s$) are as follows. In the course of heating, thermal stress occurs to the specimen, which disappears toward the wire radius within ~ 25 ns. A sound wave covers the distance between the center of a wire section and its ends within about 4 μs, which exceeds the time necessary to heat the specimen to melting. Therefore, the wire is compressed along its axis (at the imaging point equally distant from the ends). The estimation of stresses, when the imparted energy is $0.5\ kJ \cdot g^{-1}$, provides a value of about 10 to 30 kbar, which exceeds the Zr yield limit (~ 2.8 kbar). Thus, the metal plastically deforms and expands along the wire radius. Such behavior of the heated wire allows measurements of the specific volume of solid zirconium, as well as the liquid, by measuring only the wire diameter. It is quite natural that the cylindrical shape of the specimen is distorted (under such kind of deformation), which leads to nonuniform heating of the specimen and errors in measuring resistivity and energy. The deviations of temperature will be of the order of the wire cross-sectional variation. The described picture of deformation will take place when there is no bend deformation. The bend deformation should lead to different displacement of the shadowgraph boundaries, with regard to the wire central axis. In all of our experiments except one, the displacement of the boundaries is the same. This single experiment gives a displacement difference of 1 to 2 μm (at an energy of $1.67\ kJ \cdot g^{-1}$). This confirms the assumption that the bend deformation is either absent or negligible.

According to our data (Fig. 6), at a specific imparted energy of $E = 2.0\ kJ \cdot g^{-1}$, the relative expansion of zirconium, V/V_0, does not exceed 19%. To introduce the temperature value, we use the data of Fink [15] for Zr (enthalpy $H = 1.78\ kJ \cdot g^{-1}$ for $T = 4200$ K). Using these data, it is possible to calculate the average expansion coefficient of liquid zirconium (from the melting point up to 4200 K). In our experiment it turned out to be $\beta \approx 46 \times 10^{-6}\ K^{-1}$.

According to data from Ref. 11, the temperature coefficient of linear expansion of iron (solid phase) α is $\sim 20 \times 10^{-6}\ K^{-1}$ before melting. According to published data [11] for zirconium, α is $\sim 10 \times 10^{-6}\ K^{-1}$ at 1600 K. In other words, iron in the as solid state as well as in the liquid state has higher values of α and, correspondingly, of β. According to our experimental data and evaluations, the average temperature coefficient of the volumetric expansion of liquid iron β is $\sim 102 \times 10^{-6}\ K^{-1}$, and for liquid zirconium it is $\approx 46 \times 10^{-6}\ K^{-1}$.

The results of this work on liquid iron density are in reasonable agreement with other published data. The results on liquid zirconium density were obtained through direct density measurements (digital photometrical processing of the shadow picture across the wire), just as for the experimental results for iron.

ACKNOWLEDGMENTS

This work was performed under the auspices of the International Nuclear Safety Centre of the Russian Ministry of Atomic Energy (RINSC) and the U.S. International Nuclear Safety Center (USINSC) at the Argonne National Laboratory. Funding for this effort was provided by the U.S. Department of Energy. The authors would like to thank Dr. Joanne K. Fink (physicist at Argonne National Laboratory) for useful discussions and for interest in the investigations.

REFERENCES

1. G. Pottlacher, E. Kaschnitz, and H. Jäger, *J. Non-Crystal. Solids* **156–158**:374 (1993).
2. D. R. Wilson, *Liquid Metal and Alloy Structures* (Metallurgia, Moscow, 1972), p. 195.
3. W. D. Drotning, *High Temp. High Press.* **13**:441 (1981).
4. V. N. Andronov, B. V. Chekin, and S. V. Nesterenko, *Liquid Metals and Slugs* (Metallurgia, Moscow, 1977), p. 23.
5. R. S. Hixson, M. A. Winkler, and M. L. Hodgdon, *Phys. Rev. B* **42**:6485 (1990).
6. M. Beutl, G. Pottlacher, and H. Jäger, *Int. J. Thermophys.* **15**:1323 (1994).
7. N. N. Shipkov, V. I. Kostikov, E. I. Neproshin, and A. V. Demin, *Recrystallized Graphite* (Metallurgia, Moscow, 1979), p. 75.
8. V. P. Yelyutin and M. A. Maurakh, *News USSR Acad. Sci. OTN* **4**:129 (1956).
9. A. F. Guillermet, *High Temp. High Press.* **19**:119 (1987).
10. G. R. Gathers, *Int. J. Thermophys.* **4**:273 (1983).
11. V. E. Zinoviev, *Thermophysical Properties of Metals at High Temperatures* (Metallurgia, Moscow, 1989), p. 226.
12. M. E. Drits (ed.) *Properties of Elements, Vol. 1* (Metallurgia, Moscow, GUP "Tsvetnye Metally Journal," 1997), p. 252.
13. Y. S. Touloukian, R. K. Kirby, R. E. Taylor, and P. D. Desai, in *Thermophys. Prop. Matter, Vol. 12* (IFI/Plenum, New York, 1976), as indicated in Ref. 10.
14. G. B. Skinner and H. L. Johnston, *J. Chem. Phys.* **21**:1383 (1953).
15. J. K. Fink, http://www.insc.anl.gov/matprop/zirconium/zrhlf.pdf.